Measurement of 3D Left Ventricular Strains During Diastole Using Image Warping and Untagged MRI Images

AI Veress, JA Weiss, RD Rabbitt, JN Lee, GT Gullberg

University of Utah, Salt Lake City, USA

Abstract

Image based finite element analysis of the left ventricle (LV) was used to determine deformation and strain developed between mid-diastole and end-diastole. The algorithm used volumetric MRI data to create a body force that deformed a finite element model of the LV in mid-diastole into and tracks tissue deformation.

A volumetric MRI dataset corresponding to mid-diastole was designated as the reference image and an image corresponding to end-diastole was designated the deformed image. The reference image was manually segmented and a three dimensional finite element mesh was created. The Warping version of the non-linear finite element program NIKE3D (Lawrence Livermore National Laboratory) was used to analyze the images

Warping results of the left ventricular circumferential stretch measurements at the base and mid-ventricle were compared with direct measurement of image data set. Warping results showed less than 3% difference between the methods.

1. Introduction

Assessment of regional heart wall motion (wall motion, thickening, strain, etc.) can provide quantitative estimates of ventricular wall function, localize ischemic myocardial disease, and identify impairment of cardiac function due to hypertrophic or dilated cardiomyopathies. Our long-term goal is to determine the effect of these pathologies on the local wall function of the heart by determining the changes in strain distribution resulting from these conditions.

The deformation of the human heart wall has been quantified via the attachment of physical markers in a select number of human subjects [1]. This approach provided valuable information but is far too invasive to be used in the clinical setting. With the development of magnetic resonance imaging (MRI) tagging techniques, non-invasive measurements of myocardial wall dynamics have been possible [2]. The MRI tagging technique relies on local perturbation of the magnetization of the myocardium with selective radio-frequency (RF) saturation to produce multiple, thin tag planes during diastole. The resulting magnetization reference grid persists for up to 400 ms and is convected with the myocardium as it deforms. This is followed by conventional, orthogonal-plane imaging during systole [3]. The tags provide fiducials from which the deformation gradient and strain tensors can be calculated. Deformable models in the form of "snakes" or thin plate splines are often incorporated to localize the tags within the images [4]. The tags are usually laid down as a rectilinear grid, using image acquisition that is gated to the ECG to acquire multiple slices and thus form a 3D dataset.

The primary strength of MRI tagging is that noninvasive *in vivo* strain measurements are possible [5, 6]. It is effective for tracking fast, repeated motions in 3D. Probably the most significant limitations of the technique for cardiac imaging are its spatial resolution, which is much coarser than the MRI acquisition matrix, and the lengthy image acquisition time.

Sinusas *et al.* have developed a method to determine the strain distributions of the left ventricle using un-tagged MRI [7]. The system is a shaped based approach for quantifying regional myocardial deformations. The shape properties of the endo- and epicardial surfaces are used to derive 3-D trajectories which are in turn used to deform a finite element mesh of the myocardium. The approach requires a segmentation of the myocardial surfaces in each 3-D image data set to derive the surface displacements.

We have developed an image based finite element technique known as Warping that allows the extraction of strain information from sequences of images of a deforming tissue without markers. As an initial feasibility study for its application to untagged MRI images of the heart, average cicumferential stress at base and mid-ventricle locations were predicted using the Warping technique and were compared to hand measurements at corresponding locations.

0276-6547/01 $17.00 © 2001 IEEE

Computers in Cardiology 2001;28:165-168.

2. Methods

A three dimensional MRI dataset of a healthy volunteer's heart was aquired using a Marconi 1.5 Tesla scanner. The dataset consisted of 16 five-millimeter thick short axis slices. The slices were acquired with a cardiac gated sequence using 256x128 image matrix (TE=2.7 ms, bandwidth=31.3 kHz, flip angle=35°, FOV=22.5 cm). Data acquisition began 120 msec after the cardiac trigger. The sequence acquired two averageso f 4 image phases for each of 10 images acquired at different delays during the cardiac cycle. Two of the 10 images were used in the computations, corresponding to mid- and end-diastole. The acquisition time for each slice was 64 seconds. The volunteer practiced shallow breathing during image acquisition (Figures 1A,1 B).

The left ventricular lumen and epicardial surface were manually segmented to create the finite element model (Figure 1C). For this initial study, the myocardium was represented as a neo-Hookean material. The myocardial shear modulus was defined as 2.5 KPa and the bulk modulus was defined as 200.0 KPa.

2.1. Warping theory

A brief description of the approach for deformable image registration is provided below. Additional details can be found in previous publications [8, 9]. The approach requires an image of the tissue in a reference configuration (*template* image), and an image in the deformed configuration (*target* image). The Warping technique produces a position-dependent body forcef rom the pointwise intensity differences between the images. This body force is applied to a discretization of the object of interest in the template image to cause it to deform into registration with the target image. The Warping body force is derived from an image-based energy density U defined as the pointwise difference in intensities between the template and target images:

$$U(\mathbf{X},\varphi)=\frac{\lambda}{2}(T(\mathbf{X},\varphi)-S(\mathbf{X},\varphi))^2 \qquad (1)$$

Here, $\varphi(X)$ is the deformation map applied to the template image, X represents the reference coordinates of a material point in the template, T and$S$a re the scalar template and target image intensities at a point in the domain of the deformed template, and λ is a penalty parameter. The total energy of the continuum, $E(\varphi)$, is defined as the sum of the image-based energy density and the standard strain energy density for a hyperelastic material,$W(X,C)$:

$$E(\varphi)=\int_B W(\mathbf{X},\mathbf{C}(\varphi(\mathbf{X})))dV+\int_B U(\mathbf{X},\varphi(\mathbf{X}))dV \qquad (2)$$

Here,C is the right deformation tensor.

At equilibrium, the total energy in the system is minimized and the internal material forces due to the stress divergence balance with those that arise from the image-based energy term. The first variation of $E(\varphi)$ with respectt o φ yields the modified equilibrium equations for the continuum [9]. An image-based force term arises:

$$\frac{\partial U}{\partial \varphi}=\lambda(T(\mathbf{X},\varphi(\mathbf{X}))-S(\mathbf{X},\varphi(\mathbf{X})))\left(\frac{\partial T}{\partial \varphi}-\frac{\partial S}{\partial \varphi}\right) \qquad (3)$$

This vector term is a position- and deformation-dependent body force that attempts to simultaneously minimize local differences in image intensity and intensity gradients between the template and target images. The image gradients provide the local direction information for the force vector. The image data do not contribute any forces when either the difference in image intensities is zero or the difference between the image intensity gradients is zero (Equation 3).

2.2. Sequential spatial filtering

Image registration problemsa re typically ill-posed in that they do not satisfy the general conditions of existence, uniqueness, and stability in the solution with small changes in the internal data. The Warping technique is susceptible to localm inima. The registration process may get "stuck" by alignment of local image inhomogeneities that prevent global image alignment. Our computational approach was devised to first register larger image features such as object boundaries and coarse textural detail, followed by registration of fine detail. This was achieved by employing sequential spatial filtering. By evolving the "sharpness" of the image over quasi-time, one can control the influence of fine textural features in the image until global registration is achieved. Sequential spatial smoothing with a Gaussian mask was used for both the template and target images in the analyses for this study.

2.3. Warping solution procedure

The Warping analysis consisted of two phases. During thef irst phaseo f thea nalysis, the penalty parameter λ was gradually increased over quasi-time while the amount of spatial filtering remained constant, thus providing a means to evolve the image-derived forces on the model and achieve global registration of the deforming template with the target image. In the second phase, the penalty was increased at the same rate as in the first phase while the amount of spatial filtering was reduced to achieve local registration. The penalty parameterw as the largest that would allow the model to run without numerical ill-conditioning.

The changes in epicardial and endocardial circumference (average circumferential stretch) at the top

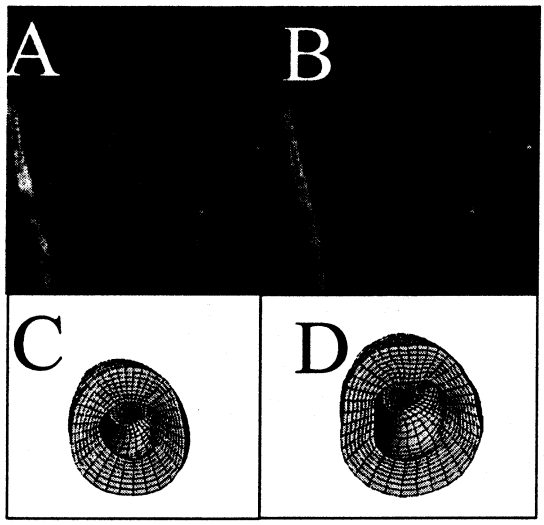

Figure 1. A - base slice oft he template image dataset representing mid-diastole. B- base slice of the target image dataset representing late-diastole. C - 3D finite element mesh of the LV based on template image dataset. D - predicted deformed geometry in late-diastole based on the Warping analysis.

slice oft he image data set (base) were measured directly from the image slices using NIH Image [10]. Similar measurements were made on the mid-ventricular slice. Three separate measurements were made at each location and the averages were used for comparison to the Warping results.

The results of the Warping analysis were used to compute similarm easurements of base and mid-ventricle circumferential stretches. The endocardial and epicardial circumferential stretch values were averaged around the circumference oft he finite element mesh forb oth slices.

Table 1. Comparison of Warping analysis stretch results with image measurements.

	Base Endocard.	Base Epicard.	Mid-Vent. Endocard.	Mid-Vent. Epicard.
Warping	1.16	1.07	1.08	1.04
Image Meas.	1.18	1.11	1.10	1.09
Difference	2.27%	2.73%	1.82%	2.89%

Stretch = deformed length/undeformed length (cm/cm)

The amount of twist at the apex was determined from the Warping results.

3. Results

There was good agreement between the Warping results and those of the manual measurements (Table 1). Differences of less than 3% were found for all locations. The Warping stretch distribution was fairly uniform throughout most of the myocardium. There are two areas

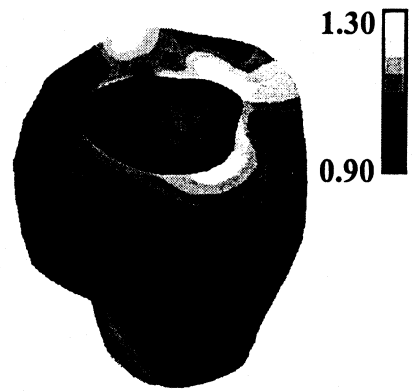

Figure 2. Predicted distribution of change in circumferential fiber stretch between mid- and late-diastole.

that appear to have high stretch (10:00 and 5:00 in Figure 2). This high stretch area is localized to the base area of the LV. The stretch distribution becomes nearly uniform by mid-ventricle. These high stretch areas may be the result of out-of-plane motion of the base of the left ventricle. Sinusas *et al.* [7] reported a similar uniform of strain distribution in the *in vivo* measurement of a canine left ventricle.

The amount of apex twist determined from Warping was 13 degrees. The amount of twist could not be measured directly from the images due to a lack of fiducial points in the image data at the apex . However, Buchalter *et al.* [6] reported epicardial apex twist values of 10-28 degrees from end-systole to end-diastole using tagged MRI. These results were consistent with results of studies that used an invasive approach[1,11]. If it is assumed that half of the twisting took place from mid-diastole to end-diastole,t he measurements from Buchalter et al. would yield 5-19 degrees of apex twist. The Warping results are within this range of apex twist.

4. Discussion

These initial results show good agreement with the imagem easurements. Whilet he results show promise, further validation work will be required before this method can be used to study the pathologies in a patient population.

We used an isotropic material model for the myocardium. While a previous validation study with intravascular ultrasound images demonstrated that Warping was relatively insensitive to material model and material parameter selection [12], a similar study should be done with MRI images of the heart. Furthermore, the effect of inhomogeneous fiber orientation must be assessed.

Warping has two advantages over tagged MRI analyses. Warping has a higher spatial resolution than tagged analysis. The finite element mesh density can be refined to near the spatial resolution of the image if sufficient computational resources are available. Furthermore, untagged image datasets require a shorter acquisition time than required for a full 3-D tagged image dataset. This is a distinct advantage for analysis of patients with myocardial damage due to myocardial infarction, orh ypertrophic and dilated cardiomyopathies, since the length of time that they may lie supine is very limited.

The shape based approach utilized by Sinusas *et al.* [7] uses a somewhat similara pproach to strain measurement without tags. However, their technique requires a segmentation for everyi mage dataset to determine the surface displacements. This is a time-consuming task. Warping only requires a segmentation of the reference (Template) dataset to generatet he finite element mesh. Further, Warping allows for virtually any material model to be used in the analysis, and accurate stress predictions can be obtained in addition to strains when an appropriate material model is used.

The present study represents an initial feasibility study to determine whether accurate results could be obtained by Warping untagged MRI image datasets. Future work will focus on additional validation of this technique,u sing the results from a "forward" finite element analysis as a gold standard for comparison. The results from this forward modelw ill be used to deform the template image to create a target image. The exacts train distribution will then be known and will be used for comparison to the Warping results. This approach was used to validate Warping for use with intravascular ultrasound [12]. Additional validation will include comparison of Warping with tagged MRI strain analysis by obtaining both tagged and untagged MRI datasets from a single healthy individual.

Acknowledgements

National Institute of Health RO1HL39792

References

[1] Ingels NB, Jr., Daughters GT, 2nd, Stinson EB, and Alderman EL. Measurement of midwall myocardial dynamics in intact man by radiography of surgically implanted markers. Circulation 1975; 52: 859-67.

[2] Ozturk C and McVeigh ER. Four-dimensional B-spline based motion analysis of tagged MR images: introduction and in vivo validation. Phys Med Biol 2000; 45: 1683-702.

[3] McVeigh ER and Zerhouni EA. Noninvasive measurement of transmural gradients in myocardial strain with MR imaging.R adiology 1991; 180: 677-83.

[4] Zerhouni EA, Parish DM, Rogers WJ, Yang A, and Shapiro EP. Human heart: tagging with MR imaging--a method for noninvasive assessment of myocardial motion. Radiology 1988; 169: 59-63.

[5] Ungacta FF, Davila-Roman VG, Moulton MJ, CuppsB P, Moustakidis P, Fishman DS, Actis R, Szabo BA, Li D, Kouchoukos NT, and Pasque MK. MRI-radiofrequency tissue tagging in patients with aortic insufficiency before and after operation.A nn Thorac Surg 1998; 65: 943-50.

[6] Buchalter MB, Weiss JL, Rogers WJ, Zerhouni EA, Weisfeldt ML, Beyar R, and Shapiro EP. Noninvasive quantification of left ventricular rotational deformation in normal humans usingm agnetic resonance imaging myocardial tagging. Circulation 1990; 81: 1236-44.

[7] Sinusas AJ, Papademetris X, Constable RT, Dione DP, Slade MD, Shi P, and Duncan JS. Quantification of 3-D regional myocardial deformation: shape-based analysis of magnetic resonance images. Am J Physiol Heart Circ Physiol 2001; 281: H698-714.

[8] Rabbitt RD, Weiss JA, Christensen GE, and Miller MI. Mapping of hyperelastic deformable templates using the finite element method. SPIE 1995; 2573: 252-265.

[9] Weiss JA, Rabbitt RD, and Bowden AE. Incorporation of medical image data in finite element models to track strain in soft tissues.S PIE 1998; 3254: 477-484.

[10]N IH Image, National Institute of Health, Bethesda Maryland.

[11]H anson DE, Daughters GT, Stinson EB, Alderman EL, Ingels NB, and Miller DC. Torsional deformation of the left ventricular midwall in human hearts with intramyocardial markers: Regional heterogeneity and sensitivity ot the inotropic effects of abrupt rate changes. Circ Res 1988; 62: 941-952.

[12]V eress AI, Weiss JA, Gullberg GT, Vince DG, and Rabbitt RD. Strain Measurement in Coronary Arteries Using Intravascular Ultrasound and Deformable Images. J Biomech Eng 2001; (in review).

Address for correspondence:
Grant T.G ullberg,P h.D.
MIRL,72 9 Arapeen Drive
Salt Lake City, UT 84108-1218,U SA
Grant.Gullberg@hsc.med.utah.edu